

Well-Designed Strategy To Construct Helical Silver(I) Coordination Polymers from Flexible Unsymmetrical Bis(pyridyl) Ligands: Syntheses, Structures, and Properties

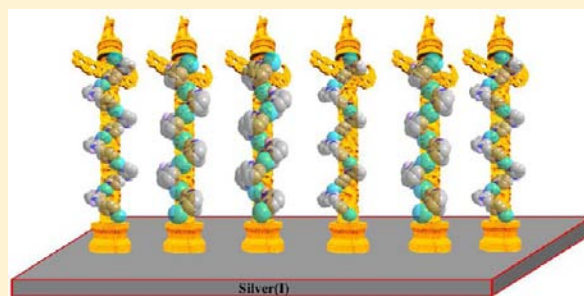
Zhu-Yan Zhang,^{†,‡} Zhao-Peng Deng,[†] Li-Hua Huo,^{*,†} Hui Zhao,[†] and Shan Gao^{*,†}

[†]Key Laboratory of Functional Inorganic Material Chemistry, Ministry of Education, Heilongjiang University, Harbin 150080, People's Republic of China

[‡]Laboratory Centre of Pharmacy, College of Pharmacy, Harbin Medical University, Harbin 150081, People's Republic of China

S Supporting Information

ABSTRACT: In this Article, self-assembly of AgX (X = NO₃⁻ and ClO₄⁻) salts and four flexible unsymmetrical bis(pyridyl) ligands, namely, *N*-(pyridin-2-ylmethyl)pyridin-3-amine (L1), *N*-(pyridin-3-ylmethyl)pyridin-2-amine (L2), *N*-(pyridin-4-ylmethyl)pyridin-2-amine (L3), and *N*-(pyridin-4-ylmethyl)pyridin-3-amine (L4), results in the formation of eight helical silver(I) coordination polymers, [Ag(L)(NO₃)_n] [L = L1 (1), L2 (2), L3 (3), L4 (4)] and [Ag(L)(ClO₄)_n] [L = L1 (5), L2 (6), L3 (7), L4 (8)], which have been characterized by elemental analysis, IR, TG, PL, and powder and single-crystal X-ray diffraction. The alternating one-dimensional (1-D) left- and right-handed helical chains are included in achiral complexes 1–3 and 5–8. By contrast, the ligand L4 only alternately bridges Ag(I) cation to form the 1-D right-handed helical chain in complex 4. The pitches of these helical chains locate in the range 5.694(5)–17.016(6) Å. Meanwhile, the present four unsymmetrical bis(pyridyl) ligands in the eight complexes present diverse *cis*–*trans* and *trans*–*trans* conformation and facilitate the construction of helical structures. Moreover, the solid-state luminescent emission intensities of the perchlorate-containing complexes are stronger than those of nitrate-containing complexes at room temperature.



INTRODUCTION

Silver(I) coordination polymers with the rigid or flexible bis(pyridyl) ligands have attracted intensive interest owing to their fascinating architectures along with the potential applications in fields of adsorption, gas storage, photoluminescence, and catalysis.^{1,2} To date, a variety of 1-D, 2-D, and 3-D bis(pyridyl) ligand based Ag(I) coordination polymers with beautiful topologies and properties have been obtained.^{3–13} However, among the plentiful 1-D motifs, the 1-D helical chain structures seem to be surprisingly sparse, which is caused by the employment of the rigid or flexible symmetrical bis(pyridyl) ligands (the symmetrical spacer attached to the same substituted position of two terminal pyridines) during the synthetic process.^{2,5a,d,10,11} In contrast to these flexible symmetrical bis(pyridyl) ligands, the flexible unsymmetrical bis(pyridyl) ligand (different substituted position of the two terminal pyridines) may be more suitable for constructing helical structures due to the fact that the unsymmetrical pyridyl rings can effectively decrease the symmetry in the unit cell and increase the freedom of distortion to form a helix.¹³ In 2008, Kitagawa and co-workers reported an Ag(I) coordination polymer, {[Ag(4-pmna)][PF₆⁻·MeOH]_n} (IV) (4-pmna = *N*-(pyridin-4-ylmethyl)nicotinamide, Scheme 1), involving flexible unsymmetrical bis(pyridyl) ligands, which crystallizes as cocrystals of IVa⊃PF₆⁻·MeOH and IVb⊃PF₆⁻·MeOH. Inter-

estingly, IVa⊃PF₆⁻·MeOH crystallizes in space group *P*₄₃ and exhibits single left-handed helical structure, while IVb⊃PF₆⁻·MeOH crystallizes in space group *P*₄₁ and exhibits single right-handed helical structure.¹³ Despite the interesting result, it is a pity that the helical Ag(I) polymers constructed from flexible unsymmetrical bis(pyridyl) ligand are scarcely reported. Hence, rational design and synthesis of Ag(I) helical polymers is still interesting and meaningful work.

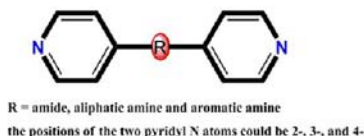
With this concept in mind, to expand our research on helical Ag(I)-bis(pyridyl) polymers,¹¹ we designed and synthesized four flexible unsymmetrical bis(pyridyl) ligands with a non-coordinating amine group in the –CH₂–NH– spacer, *N*-(pyridin-2-ylmethyl)pyridin-3-amine (L1), *N*-(pyridin-3-ylmethyl)pyridin-2-amine (L2), *N*-(pyridin-4-ylmethyl)pyridin-2-amine (L3), and *N*-(pyridin-4-ylmethyl)pyridin-3-amine (L4) (Scheme 1). The two unsymmetrical pyridyl rings can freely twist around the –CH₂–NH– group with different bond angles to meet the requirements of Ag(I) centers, and the coordination direction and different positions of the pyridyl N atoms in the four positional isomeric ligands may benefit the formation of helical structures. Meanwhile, the amine group in the flexible spacer of the four ligands can

Received: January 9, 2013

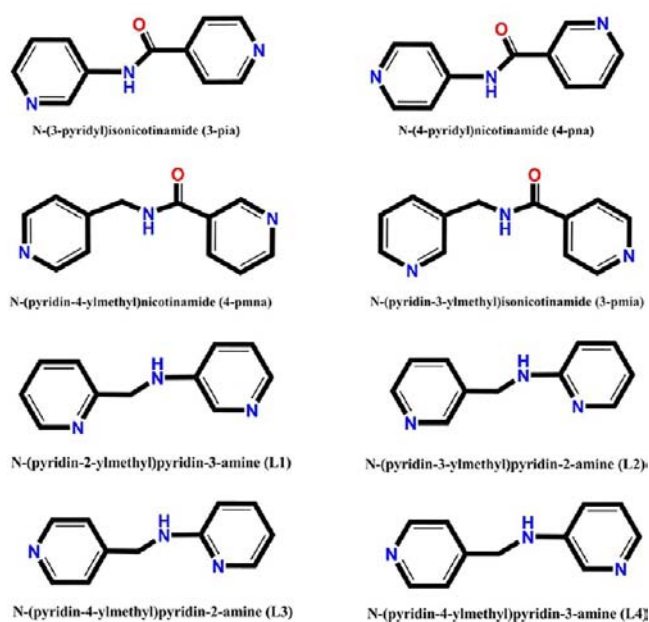
Published: May 2, 2013

Scheme 1. Symmetrical and Unsymmetrical Bis(pyridyl) Ligands in the Reported and Present Ag(I) Coordination Polymers

Symmetrical



Unsymmetrical



potentially form hydrogen bonds with the acceptor groups to facilitate the formation of helical structures and direct the self-assembly of interesting supramolecular systems. Subsequently, we reported here the syntheses, structures, and properties of eight silver(I) complexes based on the aforementioned four ligands and AgX (X = NO₃⁻ and ClO₄⁻) salts, namely, [Ag(L)(NO₃)_n] [L = L1 (1), L2 (2), L3 (3), L4 (4)] and [Ag(L)(ClO₄)_n] [L = L1 (5), L2 (6), L3 (7), L4 (8)]. As expected, the seven complexes (1–3, 5–8) contain left- and right-handed helical chains, and complex 4 contains only the right-handed helical chain. The pitches of these helical chains are varying from 5.694(5) to 17.016(6) Å with the changing of the ligands. Meanwhile, the present four unsymmetrical bis(pyridyl) ligands in the eight complexes present diverse *cis-trans* and *trans-trans* conformation and facilitate construction of helical structures. Moreover, the emission intensities of the perchlorate-containing complexes are stronger than those of nitrate-containing complexes at room temperature.

EXPERIMENTAL SECTION

General Procedures. All chemicals and solvents were of A. R. grade and used without further purification in the syntheses. L1–L4 were synthesized according to the previously reported method.¹⁴ Elemental analyses were carried out with a Vario MICRO from Elementar Analysensysteme GmbH, and the infrared spectra (IR) were recorded from KBr pellets in the range 4000–400 cm⁻¹ on a Bruker Equinox 55 FT-IR spectrometer. Powder X-ray diffraction (PXRD) patterns were measured at 293 K on a Bruker D8 diffractometer (Cu Kα, λ = 1.540 59 Å). The TG analyses were

carried out on a Perkin-Elmer TG/DTA 6300 thermal analyzer under flowing N₂ atmosphere, with a heating rate of 10 °C/min. The circular dichroism (CD) spectrum was recorded on a JASCO J-810 spectropolarimeter (JASCO, Hiroshima, Japan). The spectrum was collected on powder samples of crystal embedded in KCl pellets at a rate of 100 nm min⁻¹. Luminescence spectra were measured on a Perkin-Elmer LS 55 luminance meter.

Synthesis of [Ag(L)(NO₃)_n] (1–4). L (2 mmol) was dissolved in 10 mL methanol solution and then added to the MeCN solution containing equal amount of silver(I) nitrate. The mixture was stirred at room temperature for 10 min, and then filtered. Colorless crystals of 1–4 were isolated from the filtrate after avoiding illumination for several days.

Data for complex 1 follow: yield 63% (based on Ag). Anal. Calcd for C₁₁H₁₁N₄O₃Ag: C 37.21, H 3.12, N 15.78%. Found: C 37.24, H 3.17, N 15.75%. IR (ν/cm⁻¹): 3213m, 2926w, 1598s, 1526m, 1481m, 1382s.

Data for complex 2 follow: yield 62% (based on Ag). Anal. Calcd for C₁₁H₁₁N₄O₃Ag: C 37.21, H 3.12, N 15.78%. Found: C 37.17, H 3.07, N 15.74%. IR (ν/cm⁻¹): 3289m, 2928w, 1603s, 1523m, 1484m, 1376s.

Data for complex 3 follow: yield 57% (based on Ag). Anal. Calcd for C₁₁H₁₁N₄O₃Ag: C 37.21, H 3.12, N 15.78%. Found: C 37.25, H 3.15, N 15.81%. IR (ν/cm⁻¹): 3246m, 2932w, 1606s, 1525m, 1478m, 1380s.

Data for complex 4 follow: yield 59% (based on Ag). Anal. Calcd for C₁₁H₁₁N₄O₃Ag: C 37.21, H 3.12, N 15.78%. Found: C 37.26, H 3.18, N 15.82%. IR (ν/cm⁻¹): 3279m, 2929w, 1595s, 1526m, 1481m, 1379s.

Synthesis of [Ag(L)(ClO₄)_n] (5–8). These complexes were obtained by the same method used for the preparation of complexes 1–4 using silver(I) perchlorate instead of silver(I) nitrate. Colorless crystals of 5–8 were isolated from the filtrate after avoiding illumination for several days.

Data for complex 5 follow: yield 67% (based on Ag). Anal. Calcd for C₁₁H₁₁N₃O₄ClAg: C 33.66, H 2.82, N 10.70%. Found: C 33.61, H 2.76, N 10.67%. IR (ν/cm⁻¹): 3266m, 2928w, 1598s, 1521m, 1479m, 1092s.

Data for complex 6 follow: yield 64% (based on Ag). Anal. Calcd for C₁₁H₁₁N₃O₄ClAg: C 33.66, H 2.82, N 10.70%. Found: C 33.69, H 2.86, N 10.73%. IR (ν/cm⁻¹): 3361m, 2926w, 1604s, 1527m, 1482m, 1096s.

Data for complex 7 follow: yield 61% (based on Ag). Anal. Calcd for C₁₁H₁₁N₃O₄ClAg: C 33.66, H 2.82, N 10.70%. Found: C 33.63, H 2.78, N 10.73%. IR (ν/cm⁻¹): 3260m, 2931w, 1603s, 1523m, 1476m, 1091s.

Data for complex 8 follow: yield 65% (based on Ag). Anal. Calcd for C₁₁H₁₁N₃O₄ClAg: C 33.66, H 2.82, N 10.70%. Found: C 33.68, H 2.85, N 10.66%. IR (ν/cm⁻¹): 3216m, 2932w, 1597s, 1524m, 1481m, 1093s.

Caution! Although not encountered in our experiments, metal perchlorates are potentially explosive. They should be handled carefully.

X-ray Crystallographic Measurements. Table 1 provides a summary of the crystal data, data collection, and refinement parameters for complexes 1–8. All diffraction data were collected at 295 K on a RIGAKU RAXIS-RAPID diffractometer with graphite monochromatized Mo Kα (λ = 0.710 73 Å) radiation in ω scan mode. All structures were solved by direct method and difference Fourier syntheses. All non-hydrogen atoms were refined by full-matrix least-squares techniques on F² with anisotropic thermal parameters. The hydrogen atoms attached to carbon and nitrogen atoms were placed in calculated positions with C–H = 0.93 Å, N–H = 0.86 Å, and U(H) = 1.2U_{eq}(C, N) in the riding model approximation. All calculations were carried out with the SHELXL97 program.¹⁵ The CCDC reference numbers are 914498–914505 for complexes 1–8.

RESULTS AND DISCUSSION

Syntheses and IR Spectra. In order to investigate whether the flexible unsymmetrical bis(pyridyl) ligands are a benefit for the formation of helical structures or not, four such types of ligands with a noncoordinating amine group in the –CH₂–NH– spacer are designed and employed to synthesize silver(I) polymers with AgX (X = NO₃⁻ and ClO₄⁻) salts under the

Table 1. Crystal Data and Structure Refinement Parameters of Complexes 1–8

	1	2	3	4
empirical formula	C ₁₁ H ₁₁ N ₄ O ₃ Ag	C ₁₁ H ₁₁ N ₄ O ₃ Ag	C ₁₁ H ₁₁ N ₄ O ₃ Ag	C ₁₁ H ₁₁ N ₄ O ₃ Ag
<i>M_r</i>	355.11	355.11	355.11	355.11
cryst syst	monoclinic	monoclinic	monoclinic	orthorhombic
space group	<i>P</i> 2 ₁ / <i>c</i>	<i>P</i> 2 ₁ / <i>n</i>	<i>P</i> 2 ₁ / <i>c</i>	<i>P</i> 2 ₁ 2 ₁
<i>a</i> /Å	8.3872(4)	9.6939(19)	7.3958(15)	7.1294(3)
<i>b</i> /Å	5.6936(3)	9.5621(19)	17.016(3)	11.9506(4)
<i>c</i> /Å	25.8904(12)	13.715(3)	10.135(2)	15.2184(5)
<i>α</i> /deg	90.00	90.00	90.00	90.00
<i>β</i> /deg	100.486(4)	102.13(3)	90.60(3)	90.00
<i>γ</i> /deg	90.00	90.00	90.00	90.00
<i>V</i> /Å ³	1215.71(10)	1242.9(4)	1275.4(4)	1296.62(8)
<i>Z</i>	4	4	4	4
<i>D_c</i> /g cm ⁻³	1.940	1.898	1.849	1.819
<i>μ</i> /mm ⁻¹	1.668	1.631	1.590	1.564
<i>θ</i> range	3.67–27.55	3.03–27.44	3.00–27.48	3.17–27.55
reflns collected	5406	11 102	12 459	3201
unique reflns	2793	2827	2918	2435
no. params	172	172	173	173
<i>F</i> (000)	704	704	704	704
R1, wR2 [<i>I</i> > 2σ(<i>I</i>)]	0.0262, 0.0650	0.0610, 0.1356	0.0414, 0.0944	0.0449, 0.0745
GOF on <i>F</i> ²	1.024	1.054	1.078	1.033
largest and hole/e Å ⁻³	0.421, -0.602	0.594, -0.847	0.728, -0.743	0.443, -0.328
	5	6	7	8
empirical formula	C ₁₁ H ₁₁ N ₃ O ₄ ClAg	C ₁₁ H ₁₁ N ₃ O ₄ ClAg	C ₁₁ H ₁₁ N ₃ O ₄ ClAg	C ₂₂ H ₂₂ N ₆ O ₈ Cl ₂ Ag ₂
<i>M_r</i>	392.55	392.55	392.55	785.10
cryst syst	monoclinic	monoclinic	monoclinic	monoclinic
space group	<i>P</i> 2 ₁ / <i>c</i>	<i>P</i> 2 ₁ / <i>c</i>	<i>P</i> 2 ₁ / <i>c</i>	<i>P</i> 2 ₁ / <i>c</i>
<i>a</i> /Å	9.6867(19)	9.6773(19)	8.0592(16)	11.591(2)
<i>b</i> /Å	10.515(2)	10.423(2)	16.813(3)	16.092(3)
<i>c</i> /Å	13.614(3)	13.666(3)	10.417(2)	15.338(3)
<i>α</i> /deg	90.00	90.00	90.00	90.00
<i>β</i> /deg	108.63(3)	108.94(3)	90.19(3)	99.32(3)
<i>γ</i> /deg	90.00	90.00	90.00	90.00
<i>V</i> /Å ³	1314.0(5)	1303.8(4)	1411.5(5)	2823.2(10)
<i>Z</i>	4	4	4	4
<i>D_c</i> /g cm ⁻³	1.984	2.000	1.847	1.847
<i>μ</i> /mm ⁻¹	1.753	1.767	1.632	1.632
<i>θ</i> range	2.99–25.00	3.00–27.47	3.11–25.01	3.10–25.01
reflns collected	9644	12 663	10 827	21 578
unique reflns	2302	2988	2487	4970
no. params	181	181	181	361
<i>F</i> (000)	776	776	776	1552
R1, wR2 [<i>I</i> > 2σ(<i>I</i>)]	0.0668, 0.0864	0.0467, 0.0833	0.0639, 0.1838	0.0553, 0.1726
GOF on <i>F</i> ²	1.003	1.099	1.057	1.013
largest and hole/e Å ⁻³	0.693, -0.390	1.483, -1.673	1.302, -0.887	1.026, -0.569

same reaction conditions due to its coordination tendency to the N atom. As we expected, all eight complexes constructed from the aforementioned four ligands and Ag(I) cations present helical structures. Furthermore, NO₃⁻ and ClO₄⁻ are introduced to explore the influence of their different steric configuration on the final helical structures of the eight Ag(I)–bis(pyridyl) complexes. The results show that nitrate anion can bridge Ag(I) cations in complex 2 to form –Ag–NO₃– helical chain and even results in high dimensional architectures due to its stronger coordination ability while the weakly coordinated perchlorate anion only affords the formation of low dimensional structures. The N–H stretching vibrations for all helical silver(I) coordination polymers are falling in the region 3361–3213 cm⁻¹, in which the position of the vibrations largely

depends on the positional isomeric ligands and the extent of hydrogen bonding. The characteristic vibrations of nitrate anion in complexes 1–4 are at 1382, 1376, 1380, and 1379 cm⁻¹, whereas the characteristic vibrations of perchlorate anion in complexes 5–8 are at 1092, 1096, 1091, and 1093 cm⁻¹, respectively. For complex 4, CD spectrum was measured to confirm the chirality of the bulk materials (Supporting Information).

Structure Description of Nitrate Containing Complexes 1–4. Single-crystal X-ray analyses indicate that complexes 1–4 possess the similar composition with the molecular structure comprising of one Ag(I) cation, one ligand **L** (**L** indicating **L1**–**L4**), and one nitrate anion (Figure 1). The Ag(I) cations in the four complexes exhibit diverse coordina-

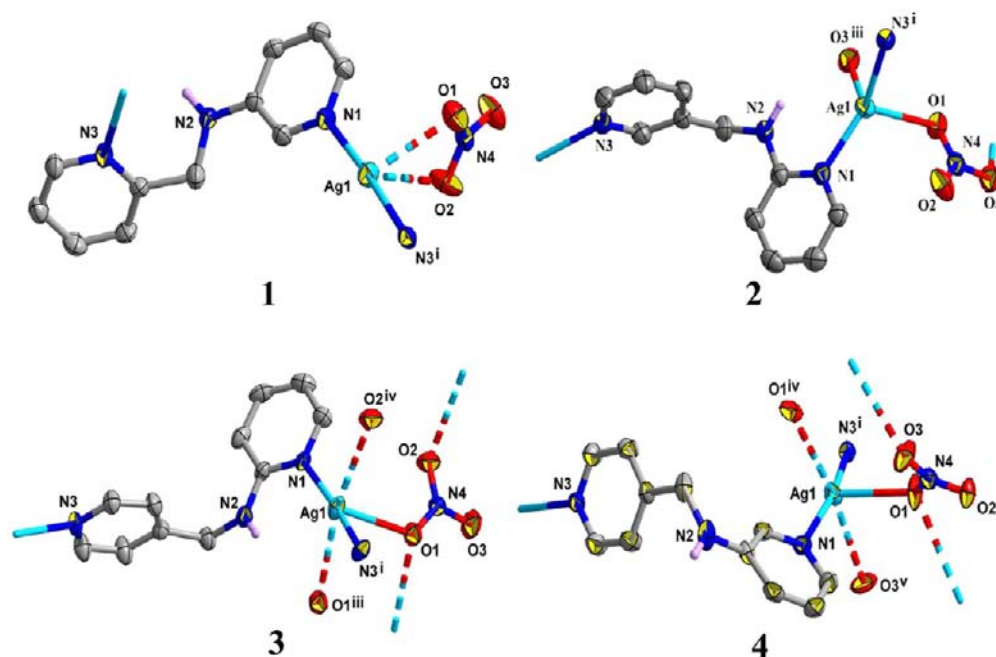


Figure 1. Perspective view of the molecular structure of complexes 1–4 showing the coordination environment around the Ag(I) cations.

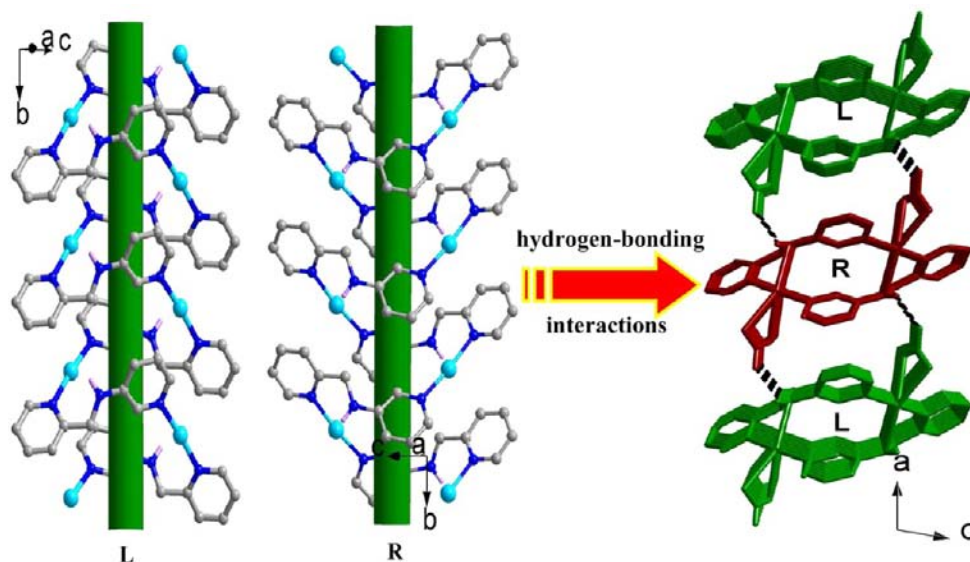


Figure 2. Left- and right-handed helical chains (left) and 2-D layer structure in complex 1.

tion spheres with the coordination numbers varying from 2 to 4. In complexes 1, 3, and 4, the Ag(I) cations are all involved in two longer contacts (2.718(2)–2.997(6) Å) to oxygen atoms of nitrate anions and exhibit linear coordination geometry in complex 1 and T-shaped coordination geometry in complexes 3 and 4. The Ag(I) cation in complex 2 is four-coordinated and presents tetrahedral coordination geometry. Despite the similarity of composition, they exhibit diverse architectures with the alteration of the different coordination modes of nitrate anion.

In complex 1, the ligand L1 adopts *trans–trans* conformation to bridge adjacent Ag(I) cations, thus giving rise to left- and right-handed helical chains as shown in Figure 2, with the nearest Ag⋯Ag distance of 6.892(5) Å in both types of helices. Interestingly, the left- and right-handed helical chains are alternately arranged through the intermolecular hydrogen-

bonding interactions between the amine groups and nitrate anions, which lead to the formation of 2-D layer motif along the *ab* plane (Figure 2).

Ligand L2 in complex 2 adopts the *cis–trans* conformation and bridges adjacent Ag(I) cations to form 1-D zigzag chain along the *c*-axis (Figure 3), in which the nearest Ag⋯Ag distance is 9.974(2) Å. Meanwhile, different from complex 1, the nitrate anions in the present complex connect adjacent Ag(I) cations in a μ_2 ($\kappa^1\text{O1}:\kappa^1\text{O3}$) bridging mode, generating a 1-D –Ag–NO₃– helical chain with the Ag⋯Ag distance being 5.718(1) Å. Subsequently, the combination of the two types of chains results in the formation of 2-D double layer structure along the *bc* plane (Figure 3), in which $\pi\cdots\pi$ stacking interactions between the N3-containing pyridyl rings are observed with the centroid-to-centroid distance being 3.628(9) Å.¹⁶ Moreover, weakly $\pi\cdots\pi$ stacking interactions

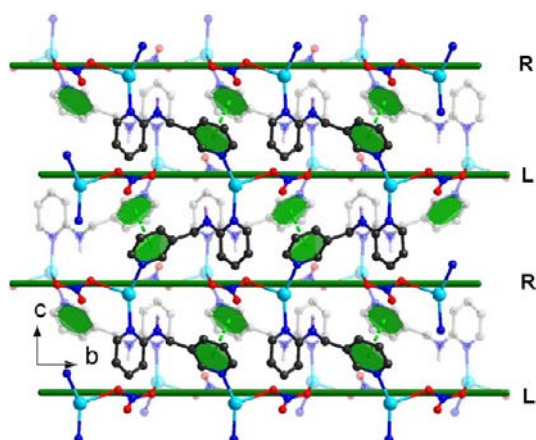


Figure 3. 2-D double layer structure of complex 2 with the black ball indicating the L2 bridged 1-D zigzag chain and the green dashed lines representing the π - π stacking interactions.

between the N1-containing pyridyl rings are also detected with the centroid-to-centroid distance being 3.884(9) Å (the upper limit for the aromatic N-containing ligand being 3.8 Å),¹⁶ which extends adjacent layers into 3-D supramolecular network as shown in Figure S1 (Supporting Information).

As observed in complex 2, the ligand L3 in complex 3 also adopts *cis-trans* conformation and bridges adjacent Ag(I) cations to give rise to left- and right-handed helical chains as shown in Figure 4, with the nearest Ag...Ag distance of

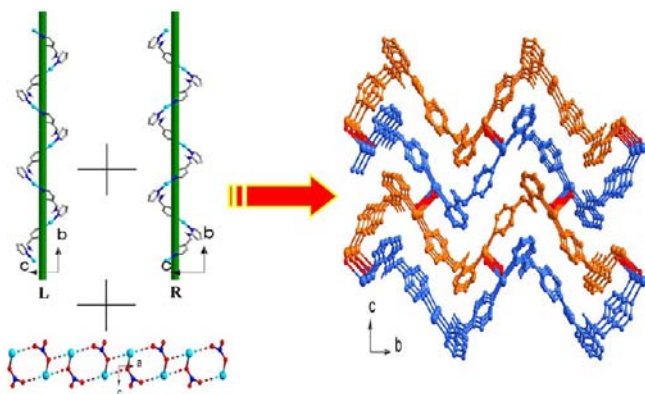


Figure 4. 3-D network of complex 3 assembled from the linkage of 1-D -Ag-NO₃- tape and helical chains.

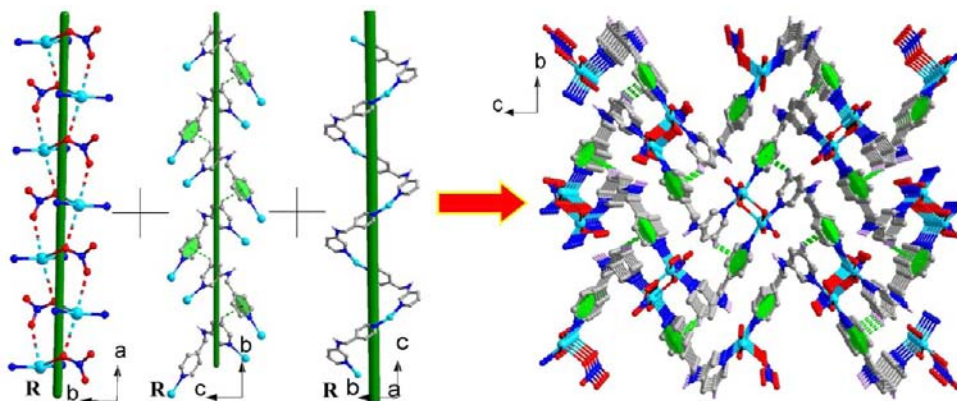


Figure 5. 3-D network of complex 4 assembled from the linkage of 1-D helical chains along *a*-, *b*-, and *c*-axis.

9.541(2) Å in both types of helices. Besides, the nitrate anions in this complex exhibit a different μ_3 ($\kappa^2\text{O}1:\kappa^1\text{O}2$) bridging mode by considering the longer contacts to Ag(I) cations. With the assistance of the nitrate anions, adjacent Ag(I) cations are extended into 1-D tape along the *a*-axis which contains alternate four- and eight-membered rings Ag₂O₂ and Ag₂O₄N₂ (Figure 4). The Ag...Ag separations in the two types of rings are 4.391(1) and 5.206(1) Å, respectively. Then, the 1-D tape connects adjacent 1-D left- and right-handed helical chains to form 3-D network (Figure 4).

Different from complexes 1–3, complex 4 crystallizes in chiral space group $P2_12_12_1$, in which the ligand L4 presents the *cis-trans* conformation and bridges adjacent Ag(I) cations to form 1-D right-handed helical chain along the *c*-axis with the nearest Ag...Ag distance being 9.054(7) Å (Figure 5). Meanwhile, the nitrate anions in this complex also exhibit μ_3 ($\kappa^2\text{O}1:\kappa^1\text{O}3$) bridging mode by considering the longer contacts to Ag(I) cations, thus connecting adjacent Ag(I) cations to generate another 1-D right-handed helical chain as shown in Figure 5. Moreover, the C–H... π interactions (C4–H4A... π , 3.786(8) Å, $\angle\text{C–H}\cdots\pi = 137.8^\circ$) between the π electron density of pyridyl ring and adjacent CH group are observed,¹⁷ which then extend adjacent [Ag₂(L)]²⁺ unit into the third 1-D right-handed helical chain. Therefore, the combination of the three types of helical chains at the points of Ag(I) cations leads to the formation of the 3-D network (Figure 5).

Structure Description of Perchlorate Containing Complexes 5–8. As shown in Figure 6, complexes 5–7 possess the similar composition with the molecular structure comprising one Ag(I) cation, one ligand L, and one perchlorate anion. By contrast, the molecular structure of complex 8 contains two Ag(I) cations, two ligands L, and two perchlorate anions. Different from the nitrate containing complexes, the four perchlorate containing complexes all present 1-D helical structures, and the Ag(I) cations in complexes 5–8 exhibit linear coordination geometry with one or two longer contacts (2.825(1)–2.951(6) Å) to oxygen atoms of perchlorate anions. Various weak interactions involving perchlorate anion lead to the formation of diverse architectures in the present four complexes.

Different from complex 1, the ligand L1 in complex 5 adopts *cis-trans* conformation to bridge adjacent Ag(I) cations, thus giving rise to left- and right-handed helical chains as shown in Figure 7. Owing to the conformational difference of the ligand, the nearest Ag...Ag distance of 7.730(2) Å in the present two types of helices is longer than that in complex 1. As shown in

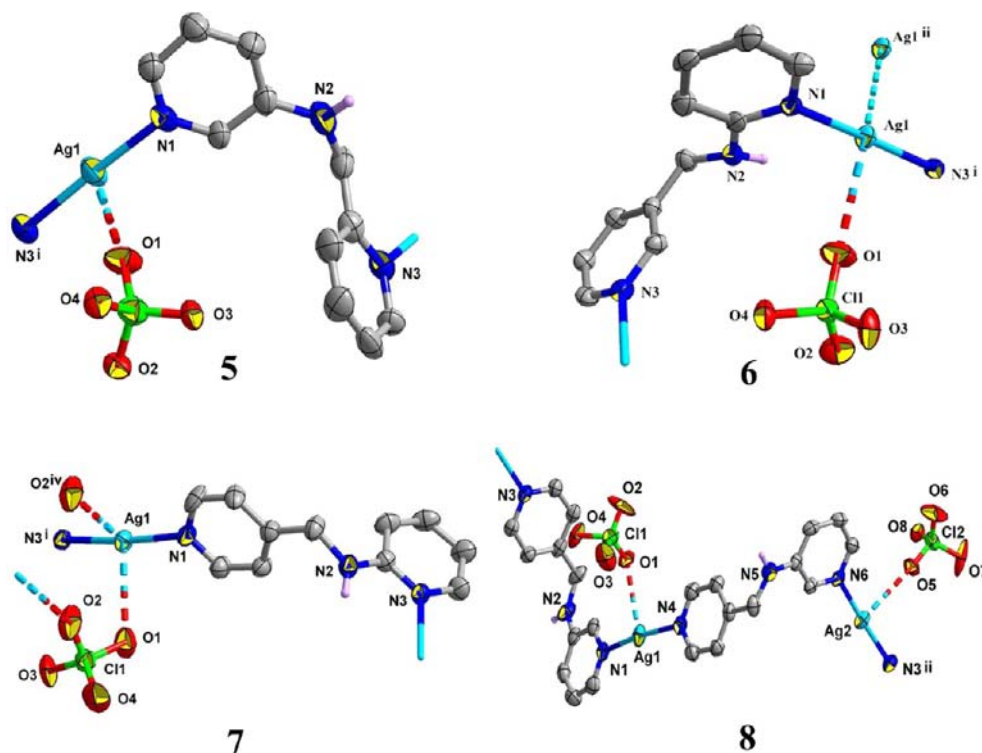


Figure 6. Perspective view of the molecular structure of complexes 5–8 showing the coordination environment around the Ag(I) cations.

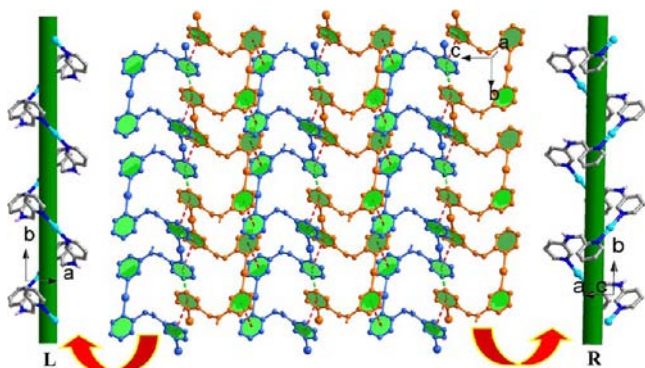


Figure 7. 2-D layer structure of complex 5 extended by the $\pi\cdots\pi$ stacking interactions. Blue and orange ball-and-stick modes indicate the left- and right-handed helical chains.

Figure 7, adjacent helices arrange alternately along the bc plane with the pyridyl rings intercrossed with each other, which then afford the formation of the $\pi\cdots\pi$ stacking interactions. A close inspection reveals that there are two types of $\pi\cdots\pi$ stacking interactions.¹⁶ One exists between N1- and N3-containing pyridyl rings with the centroid-to-centroid distance being 3.574(5) Å, while the other exists between two N3-containing pyridyl rings with the centroid-to-centroid distance being 3.889(7) Å. Therefore, adjacent helices are extended into 2-D layer motif by the aforementioned $\pi\cdots\pi$ stacking interactions. Moreover, weakly $\pi\cdots\pi$ stacking interactions between the N1-containing pyridyl rings are also detected with the centroid-to-centroid distance being 3.785(6) Å,¹⁶ which further extends adjacent layers into 3-D supramolecular network as shown in Figure S2 (Supporting Information).

Complex 6 is isostructural with complex 5. The ligand L2 in complex 6 exhibits the *cis-trans* conformation as in complex 2 and bridges adjacent Ag(I) cations to form left- and right-

handed helical chains instead of 1-D zigzag chain in complex 2 (Figure 8). The nearest Ag \cdots Ag distance of 7.524(2) Å in the present two types of helices is comparable to those in complex 5 due to their similar dihedral and axis angles (Table 2). Also, the left- and right-handed helical chains arrange alternately along the bc plane with the pyridyl rings intercrossed with each other, which then afford the formation of the 2-D layer motif (Figure 8) with the $\pi\cdots\pi$ stacking interactions between N1- and N3-containing pyridyl rings (the centroid-to-centroid distance being 3.541(5) Å).¹⁶ Meanwhile, weak Ag \cdots Ag interactions between the Ag(I) cations in the two types of helices are also observed with the separation being 3.293(1) Å. Furthermore, weakly $\pi\cdots\pi$ stacking interactions between the N3-containing pyridyl rings are detected with the centroid-to-centroid distance being 3.715(6) Å,¹⁶ which further extends adjacent layers into 3-D supramolecular network as shown in Figure S3 (Supporting Information).

As observed in complex 3, ligand L3 in complex 7 also adopts *cis-trans* conformation and bridges adjacent Ag(I) cations to give rise to left- and right-handed helical chains as shown in Figure 9, with the nearest Ag \cdots Ag distance of 9.755(2) Å in both two types of helices being comparable to those in complex 3. Subsequently, the left- and right-handed helical chains are interconnected alternately by the weakly coordinated perchlorate anions to give rise to 2-D (4,4) layer by considering the [Ag₂(ClO₄)₂] dinuclear as 4-c node (Figure 9). Moreover, the O1 atoms of the terminal coordinated perchlorate anions form intermolecular hydrogen bonding interactions with the amine groups (N2–H2N), which result in 3-D supramolecular network as shown in Figure S4 (Supporting Information).

The two *cis-trans* conformational ligand L4 in complex 8 bridges adjacent Ag(I) cations to form left- and right-handed helical chains (Figure 10), in which the nearest Ag \cdots Ag distance in the two types of helices is 8.929(2) Å. Subsequently, adjacent

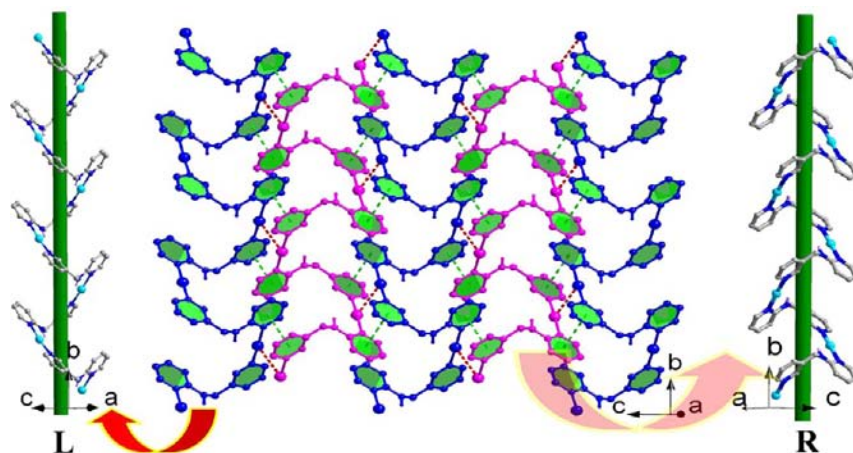


Figure 8. 2-D layer structure of complex **6** extended by the $\pi\cdots\pi$ stacking interactions. Blue and pink ball-and-stick modes indicate the left- and right-handed helical chains.

Table 2. Conformations of the Four Flexible Unsymmetrical Bis(pyridyl) Ligands

ligand	complex	conformation ^a	dihedral angle/deg	axis angle ^b /deg	Ag(I) \cdots Ag(I) distances /Å
L1	1	<i>trans-trans</i>	65.84	83.63	6.892(5)
	5	<i>cis-trans</i>	78.80	86.23	7.730(2)
L2	2	<i>cis-trans</i>	80.22	34.68	9.974(2)
	6	<i>cis-trans</i>	78.52	88.52	7.524(2)
L3	3	<i>cis-trans</i>	87.18	85.34	9.541(2)
	7	<i>cis-trans</i>	88.28	74.16	9.755(2)
L4	4	<i>cis-trans</i>	86.23	81.97	9.054(5)
		<i>cis-trans</i> (N1)	87.23	82.20	8.929(2)
	<i>cis-trans</i> (N4)	87.06	84.12	9.049(2)	

^aThe former are defined by the position of the pyridine ring: located at the opposite side of the $-\text{CH}_2-\text{NH}-$ line is *trans* while the same side is *cis*; the latter are defined by the orientation of the N atoms in the pyridine ring: pointed at the opposite direction is *trans* while the same direction is *cis*. ^bAxis angle refers to the angle between the two Ag–N bonds.

left- and right-handed helical chains are extended into 2-D layer motif through the weak Ag \cdots Ag interactions (Ag1 \cdots Ag1ⁱ, 3.242(1) Å; Ag2 \cdots Ag2ⁱⁱⁱ, 3.217(1) Å).¹⁸ Meanwhile, it should be noted that anion $\cdots\pi$ interactions (the distance between the closest oxygen atom and the centroid of the phenyl ring being 3.188(9) Å, plan-centroid-anion angle = 88.5°) between the perchlorate anions and the π electron density of N4-containing pyridyl ring are observed,¹⁷ which further stabilize the 2-D layer (Figure 10). Furthermore, the terminal coordinated perchlorate anions form intermolecular hydrogen bonding interactions with the amine groups, which result in 3-D supramolecular network as shown in Figure S5 (Supporting Information).

Influence of the Anions on the Architectures. From the aforementioned description, complexes **1** and **3–8** present $-\text{Ag}-\text{L}-$ helical chains while complex **2** exhibits $-\text{Ag}-\text{NO}_3-$ helical chain. However, the different nature of the two types of inorganic anions has influence on the coordination spheres of Ag(I) cation and final extended architectures. On one hand, for the nitrate-containing complexes **1–4**, the stronger coordinated nitrate anion involves in the coordination environment of the Ag(I) cations and makes the Ag(I) cations in the four complexes exhibit diverse coordination spheres from linear, T-shaped, to tetrahedral coordination geometry with the

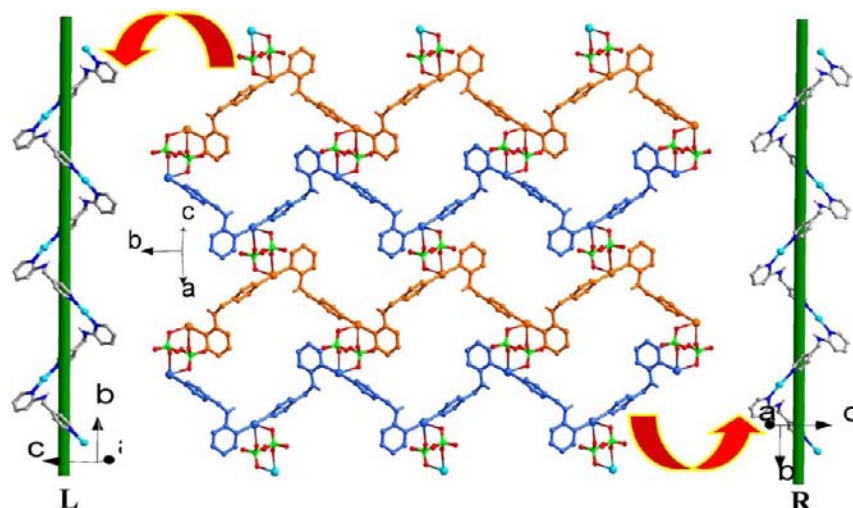


Figure 9. 2-D layer structure of complex **7** containing alternate left- (orange) and right-handed (blue) helical chains.

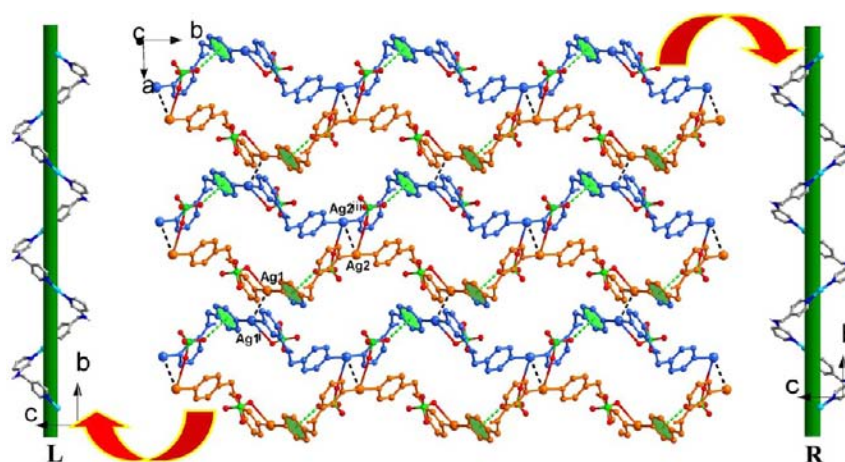


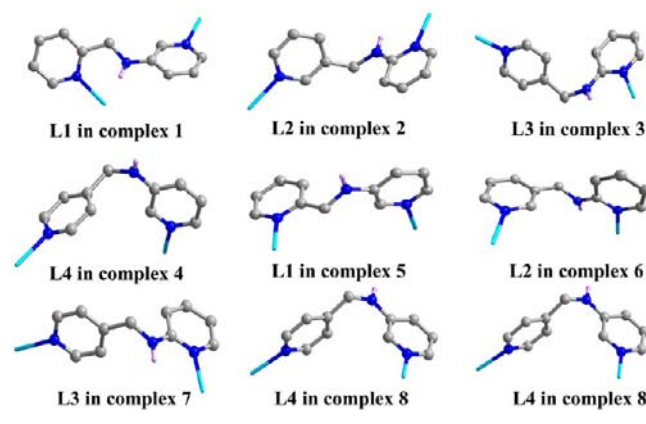
Figure 10. 2-D layer structure of complex **8** extended by the anion $\cdots\pi$ (green dashed lines) and Ag \cdots Ag (black dashed lines) interactions. Orange and blue ball-and-stick modes indicate the left- and right-handed helical chains.

coordination numbers varying from 2 to 4. In comparison, the perchlorate anion exhibits weak coordination ability, and all the Ag(I) cations in the perchlorate-containing complexes **5–8** exhibit linear coordination geometry with two coordinated N atoms from L1–L4. On the other hand, the bridging of the nitrate anion extends the 1-D –Ag–L– zigzag chain in complex **2** and 1-D –Ag–L– helical chains in complexes **3** and **4** into 2-D layer motif and 3-D network, respectively. However, complexes **5–8** are all containing 1-D –Ag–L– helical chain motifs, which are further extended into diverse architectures through the connection of various weakly interactions involving perchlorate anion. In this two types of complexes, complexes **4** and **8** exhibit clearly difference in their packing, which can be selected as representative to make further explanation. In complex **4**, the coordination and planarity of nitrate anion (a coordination bond and two weakly interacts to Ag(I) cation) make the adjacent right-handed helical chains arrange in parallel. Such arrangement facilitates the formation of C–H $\cdots\pi$ interactions and right-handed helical chains in three directions (Figure 5). By contrast, the perchlorate anion in complex **8** only presents a weak contact to Ag(I) cation. Hence, such a weak interaction cannot effectively restrict the arrangement of the helical chains and lead to the intersection of the left- and right-handed helical chains. Meanwhile, owing to the tetrahedral configuration of the perchlorate, the other three oxygen atoms of the perchlorate form anion $\cdots\pi$ and N–H \cdots O interactions with the ligand L4, which further consolidate the intersectant arrangement and result in the difference from complex **4**. Therefore, it can be concluded that the perchlorate anion is more suitable for the formation of helical structures than nitrate anion.

Influence of the Ligands on the Helical Structures. As depicted above, the reported 1-D helical chain structures constructed from the rigid or flexible symmetrical bis(pyridyl) ligands were obtained occasionally. However, in our present work, we designed and synthesized four flexible unsymmetrical ligands and reported here seven –Ag–L– helical structures and one –Ag–NO₃– helical chain. Hence, the present results demonstrate that flexible unsymmetrical ligands are prone to form helical structures. At the same time, the helical structures of the eight complexes are also influenced by the conformations and the different positions of the pyridyl N atoms in the four positional isomeric unsymmetrical bis(pyridyl) ligands. Table 2 lists the conformations of the four bis(pyridyl) ligands in the

present eight complexes. Owing to the flexibility of the four ligands, two pyridyl rings can rotate freely around the –CH₂–NH– spacer with different angles to form *cis*- and *trans*-conformations (Scheme 2), which exhibit the special ability to

Scheme 2. Diverse Conformations of the Four Unsymmetrical Bis(pyridyl) Ligands in Complexes 1–8



coordinate to silver centers and lead to interesting structure motifs. For complexes **1** and **5**, although they all contains helical chains, the different *trans–trans* and *cis–trans* conformations of L1 result in the distinct helical pitch of 5.694(5) and 10.515(1) Å, which then lead to the formation of different 3-D supramolecular network. The ligand L2 in complexes **2** and **6** acts in the same *cis–trans* conformation with the similar dihedral angles between the two pyridine rings being 80.22° and 78.52°, respectively. However, the axis angle between the two Ag–N bonds in complex **2** of 34.68° is obviously smaller than that of 88.52° in complex **6** (Table 2), which leads to the diverse 1-D zigzag chain in complex **2** and 1-D helical chain in complex **6** with the pitch of 10.423(9) Å. The ligand L3 in complexes **3** and **7** exhibits the same *cis–trans* conformation with the comparable axis angles of 85.34° and 74.16° (Table 2). Hence, the two complexes show the similar 1-D helical chain motif and comparable helical pitch (17.016(6) and 16.813(1) Å). As the case for ligand L3, ligand L4 in complexes **4** and **8** also exhibits the same *cis–trans* conformation with the comparable dihedral and axis angles (Table 2), which then result in the formation of the similar 1-D

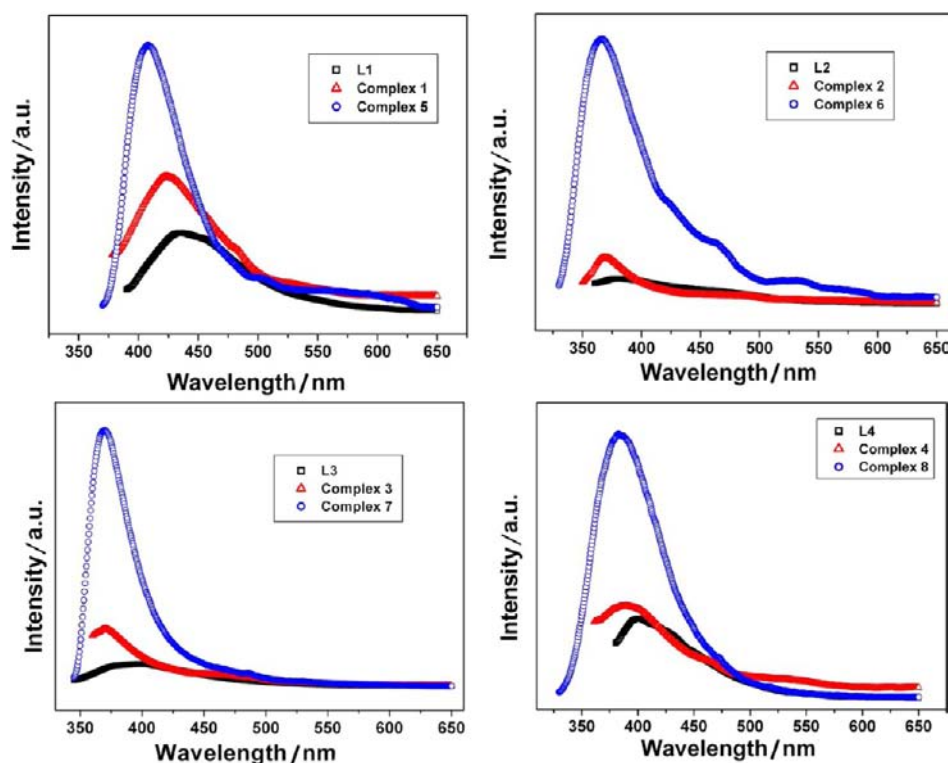


Figure 11. Emission spectra of the four free ligands and complexes 1–8 in the solid state at room temperature.

helical chain motif and comparable helical pitch (15.218(8) and 16.092(6) Å). Furthermore, from Table 2, we can also find that the bigger axis angles (larger than 74° here) can usually result in helical chains in any conformations. Meanwhile, the different positions of the pyridyl N atoms in the four positional isomeric unsymmetrical bis(pyridyl) ligands can cause subtle differences of these complexes. As observed in Table 2, with the change of the positions of the pyridyl N atoms, the Ag⋯Ag separations show a regular increasing with the sequence of L1, L2, L4, and L3. Except for the above-mentioned two points, the uncoordinated amine group (N2–H2N in all the eight complexes) in the flexible spacer of the four ligands forms hydrogen bonds with the nitrate or perchlorate O atoms (Table S2 in Supporting Information) to facilitate the formation of helices. In comparison with the ligands used by Kitagawa and co-workers,¹³ the present four flexible unsymmetrical bis(pyridyl) ligands are more able to form helical structures.

Luminescent Property. The luminescent properties of complexes 1–8 and the four free ligands in the solid state at room temperature were investigated, in which the emission spectrum of ligand L2 has been reported in our previous work.¹⁹ As shown in Figure 11, the four free ligands present emission maximum at 428, 380, 398, and 402 nm upon excitation at 372, 328, 349, and 361 nm, respectively, which could probably be attributed to the $\pi^*-\pi$ transitions.

As shown in Figure 11, upon different excitation ($\lambda_{\text{ex}} = 363$ nm for 1, 330 nm for 2, 334 nm for 3, 361 nm for 4, 352 nm for 5, 322 nm for 6, 328 nm for 7, and 355 nm for 8), complexes 1–8 exhibit emission maximum at 423, 371, 370, 390, 408, 367, 369, and 382 nm, respectively. In contrast to the emission of their corresponding free ligands, the luminescent emission band of the eight complexes can probably be assigned to the intraligand (IL) $\pi-\pi^*$ transitions because of their resemblance of the emission spectra (Figure 11).²⁰ Meanwhile, the emission

spectra of the eight complexes show various degrees of blue shift in comparison with their corresponding ligands. This could be ascribed to the fact that the conformation and the different positions of the pyridyl N atoms in the four positional isomeric unsymmetrical bis(pyridyl) ligands influence the final architectures, which further change the charge transition energy between lowest excited state and ground state. Moreover, it is interesting to note that the emission intensities for these complexes present a regular increase with the sequence of free ligands, nitrate-containing complexes, and perchlorate-containing complexes. The increasing intensity of the complexes is probably attributable to the formation of the polymeric structures, which effectively restrict the flexibility and increase the rigidity of the free ligands, thus reducing the loss of energy.²¹ Especially, the sharp increase of emission intensity for perchlorate-containing complexes could be ascribed to the anion $\cdots\pi$ and $\pi\cdots\pi$ interactions in these complexes, as well as the abundant electrons in the delocalized Π_5^8 of ClO_4^- (delocalized Π_4^6 in NO_3^-), which are preferable to increase the chance of intraligand charge transfer and the quantum efficiency.²¹

CONCLUSIONS

In conclusion, self-assembly of four flexible unsymmetrical bis(pyridyl) ligands and different AgX (X = NO_3^- and ClO_4^-) salts leads to the formation of eight helical Ag(I)-bis(pyridyl) polymers, in which the present four unsymmetrical bis(pyridyl) ligands exhibit diverse *cis-trans* and *trans-trans* conformation and facilitate construction of helical structures. Meanwhile, the different nature of the two types of inorganic anions has influence on the coordination spheres of Ag(I) cation and final extended architectures. Moreover, the solid-state luminescent emission intensities of the perchlorate-containing complexes are stronger than those of nitrate-containing complexes at room

temperature. The present result indicates that the flexible unsymmetrical bis(pyridyl) ligands can definitely be used to construct 1-D helical chain structures through rational design. Further studies on the syntheses, structures, and properties of the helical structures constructed from other flexible unsymmetrical ligands are also underway in our laboratory.

■ ASSOCIATED CONTENT

■ Supporting Information

Additional figures, PXRD patterns, TG curves, CD spectrum, selected bond distances, and selected hydrogen bond parameters for complexes 1–8, as well as X-ray crystallographic files in CIF format. This material is available free of charge via the Internet at <http://pubs.acs.org>.

■ AUTHOR INFORMATION

Corresponding Author

*E-mail: shangao67@yahoo.com (S.G.).

Notes

The authors declare no competing financial interest.

■ ACKNOWLEDGMENTS

This work is financially supported by the Key Project of Natural Science Foundation of Heilongjiang Province (No. ZD200903), Key Project of Education bureau of Heilongjiang Province (No. 12511z023, No. 2011CJHB006), and the Innovation team of Education bureau of Heilongjiang Province (No. 2010td03). We thank the University of Heilongjiang (Hdtd2010-04) for supporting this study.

■ REFERENCES

- (1) Li, J. R.; Bu, X. H.; Jiao, J.; Du, W. P.; Xu, X. H.; Zhang, R. H. *J. Chem. Soc., Dalton Trans.* **2005**, 464.
- (2) Leong, W. L.; Vittal, J. J. *Chem. Rev.* **2011**, *111*, 688.
- (3) (a) Maekawa, M.; Konaka, H.; Suenaga, Y.; Kuroda-Sowa, T.; Munakata, M. *J. Chem. Soc., Dalton Trans.* **2000**, 4160. (b) Halder, G. J.; Neville, S. M.; Kepert, C. J. *CrystEngComm* **2005**, *7*, 266. (c) Kennedy, A. R.; Brown, K. G.; Duncan, G.; Kirkhouse, J. B.; Kittner, M.; Major, C.; McHugh, C. J.; Murdoch, P.; Smith, W. E. *New J. Chem.* **2005**, *29*, 826.
- (4) (a) Dong, Y. B.; Wang, H. Y.; Ma, J. P.; Huang, R. Q. *Cryst. Growth Des.* **2005**, *5*, 789. (b) Wu, H. C.; Thanasekaran, P.; Tsai, C. H.; Wu, J. Y.; Huang, S. M.; Wen, Y. S.; Lu, K. L. *Inorg. Chem.* **2006**, *45*, 295.
- (5) (a) Withersby, M. A.; Blake, A. J.; Champness, N. R.; Hubberstey, P.; Li, W.-S.; Schröder, M. *Angew. Chem., Int. Ed.* **1997**, *36*, 2327. (b) Withersby, M. A.; Blake, A. J.; Champness, N. R.; Cooke, P. A.; Hubberstey, P.; Li, W.-S.; Schröder, M. *Cryst. Eng.* **1999**, *2*, 123. (c) Blake, A. J.; Baum, G.; Champness, N. R.; Chung, S. S. M.; Cooke, P. A.; Fenske, D.; Khlobystov, A. N.; Lemenovskii, D. A.; Li, W.-S.; Schröder, M. *J. Chem. Soc., Dalton Trans.* **2000**, 4285. (d) Khlobystov, A. N.; Blake, A. J.; Champness, N. R.; Lemenovskii, D. A.; Majouga, A. G.; Zyk, N. V.; Schröder, M. *Coord. Chem. Rev.* **2001**, *222*, 155.
- (6) (a) Guo, D.; He, C.; Duan, C.-Y.; Qian, C.-Q.; Meng, Q.-J. *New J. Chem.* **2002**, *26*, 796. (b) Chen, X.-D.; Mak, T. C. W. *Dalton Trans.* **2005**, 3646.
- (7) (a) He, C.; Duan, C. Y.; Fang, C. J.; Meng, Q. J. *J. Chem. Soc., Dalton Trans.* **2000**, 2419. (b) Schmaltz, B.; Jouaiti, A.; Hosseini, M. W.; Cian, A. D. *Chem. Commun.* **2001**, 1242. (c) Horikoshi, R.; Mochida, T.; Maki, N.; Yamada, S.; Moriyama, H. *J. Chem. Soc., Dalton Trans.* **2002**, 28. (d) Applegarth, L.; Clark, N.; Richardson, A. C.; Parker, A. D. M.; Radosavljevic-Evans, I.; Goeta, A. E.; Howard, J. A. K.; Steed, J. W. *Chem. Commun.* **2005**, 5423.
- (8) (a) Tong, M.-L.; Wu, Y.-M.; Ru, J.; Chen, X.-M.; Chang, H.-C.; Kitagawa, S. *Inorg. Chem.* **2002**, *41*, 4846. (b) Catalano, V. J.; Moore, A. L. *Inorg. Chem.* **2005**, *44*, 6558. (c) Zheng, Y.; Li, J. R.; Du, M.; Zou, R. Q.; Bu, X. H. *Cryst. Growth Des.* **2005**, *5*, 215. (d) Hanton, L. R.; Young, A. G. *Cryst. Growth Des.* **2006**, *6*, 833. (e) Burchell, T. J.; Eisler, D. J.; Puddephatt, R. J. *Cryst. Growth Des.* **2006**, *6*, 974. (f) Wang, Z.-B.; Zhu, H.-F.; Zhao, M.; Li, Y.-Z.; Okamura, T.; Sun, W.-Y.; Chen, H.-L.; Ueyama, N. *Cryst. Growth Des.* **2006**, *6*, 1420. (g) Sagué, J. L.; Fromm, K. M. *Cryst. Growth Des.* **2006**, *6*, 1566. (h) Del Piero, S.; Fedele, R.; Melchior, A.; Portanova, R.; Tolazzi, M.; Zangrando, E. *Inorg. Chem.* **2007**, *46*, 4683. (i) Chen, H. C.; Hu, H. L.; Chan, Z. K.; Yeh, C. W.; Jia, H. W.; Wu, C. P.; Chen, J. D.; Wang, J. C. *Cryst. Growth Des.* **2007**, *7*, 698. (j) Zeng, J.-P.; Zhang, S.-M.; Zhang, Y.-Q.; Tao, Z.; Zhu, Q.-J.; Xue, S.-F.; Wei, G. *Cryst. Growth Des.* **2010**, *10*, 4509.
- (9) (a) Wang, Y.; Ouyang, X. M.; Okamura, T.; Sun, W. Y.; Ueyama, N. *Inorg. Chim. Acta* **2003**, *353*, 68. (b) Zhu, H. F.; Kong, L. Y.; Okamura, T. A.; Fan, J.; Sun, W. Y.; Ueyama, N. *Eur. J. Inorg. Chem.* **2004**, 1465. (c) Fielden, J.; Long, D. L.; Evans, C.; Cronin, L. *Eur. J. Inorg. Chem.* **2006**, 3930. (d) Effendy, N.; Marchetti, F.; Pettinari, C.; Skelton, B. W.; White, A. H. *Inorg. Chim. Acta* **2007**, *360*, 1424. (e) Sengupta, P.; Henkes, A. E.; Kumar, M. K.; Zhang, H.; Son, D. Y. *Synthesis* **2008**, 79. (f) Zhang, Y.; Xiang, L.; Wang, Q.; Duan, X.-F.; Zi, G. *Inorg. Chim. Acta* **2008**, *361*, 1246.
- (10) (a) Sarkar, M.; Biradha, K. *CrystEngComm* **2004**, *6*, 310. (b) Argent, S. P.; Adams, H.; Harding, L. P.; Riis-Johannessen, T.; Jeffery, J. C.; Ward, M. D. *New J. Chem.* **2005**, *29*, 904. (c) Dong, Y. B.; Sun, T.; Ma, J. P.; Zhao, X. X.; Huang, R. Q. *Inorg. Chem.* **2006**, *45*, 10613. (d) Zeng, J.-P.; Cong, H.; Chen, K.; Xue, S.-F.; Zhang, Y.-Q.; Zhu, Q.-J.; Liu, J.-X.; Tao, Z. *Inorg. Chem.* **2011**, *50*, 6521.
- (11) Deng, Z.-P.; Zhu, L.-N.; Gao, S.; Huo, L.-H.; Ng, S. W. *Cryst. Growth Des.* **2008**, *8*, 3277.
- (12) (a) Uemura, K.; Kitagawa, S.; Fukui, K.; Saito, K. *J. Am. Chem. Soc.* **2004**, *126*, 3817. (b) Ma, Y.-T.; Zhao, Q.-H. *Acta Crystallogr.* **2008**, *E64*, m110. (c) Ma, Y.-T.; Sun, B.-W.; Ng, S. W. *Acta Crystallogr.* **2008**, *E64*, m470. (d) Moon, S.-H.; Kim, T. H.; Park, K.-M. *Acta Crystallogr.* **2011**, *E67*, m1769.
- (13) Uemura, K.; Kumamoto, Y.; Kitagawa, S. *Chem.—Eur. J.* **2008**, *14*, 9565.
- (14) Foxon, S. P.; Walter, O.; Schindler, S. *Eur. J. Inorg. Chem.* **2002**, 111.
- (15) Sheldrick, G. M. *SHELXTL-97, Program for Crystal Structure Solution and Refinement*; University of Gottingen: Gottingen, Germany, 1997.
- (16) Janiak, C. *J. Chem. Soc., Dalton Trans.* **2000**, 3885.
- (17) Deng, Z.-P.; Qi, H.-L.; Huo, L.-H.; Zhao, H.; Gao, S. *CrystEngComm* **2011**, *13*, 6632.
- (18) Bondi, A. J. *J. Phys. Chem.* **1964**, *68*, 441.
- (19) Deng, Z.-P.; Zhang, Z.-Y.; Huo, L.-H.; Ng, S. W.; Zhao, H.; Gao, S. *CrystEngComm* **2012**, *14*, 6548.
- (20) (a) Alcock, N. W.; Barker, P. R.; Haider, J. M.; Hannon, M. J.; Painting, C. L.; Pikramenon, Z.; Plummer, E. A.; Rissanen, K.; Saarenketo, P. *J. Chem. Soc., Dalton Trans.* **2000**, 1447. (b) Collin, J. P.; Dixon, I. M.; Sauvage, J. P.; Williams, J. A. G.; Barigelletti, F.; Flamigni, L. *J. Am. Chem. Soc.* **1999**, *121*, 5009. (c) Xiong, R. G.; Zuo, J. L.; You, X. Z.; Fun, H. K.; Raj, S. S. S. *Organometallics* **2000**, *19*, 4183.
- (21) Rendell, D. *Fluorescence and Phosphorescence*; Wiley: New York, 1987.